XLIII CILAMCE
21–25, November, 2022
FOZ DO IGUAÇU – PR – BRAZIL

Assessment of the distortion-induced fatigue strength in steel-concrete composite bridges welded joints

Vencislau M. Quissanga[1], Guilherme S. Alencar[2], José Guilherme S. da Silva[1]

[1]*Civil Engineering Postgraduate Programme (PGECIV), State University of Rio de Janeiro (UERJ)*
São Francisco Xavier St., 524, Maracanã, 20550-900, Rio de Janeiro/RJ, Brazil
venmanquissan@gmail.com, jgss@uerj.br
[2]*Civil and Environmental Engineering Department. University of Brasilia (UnB)*
Campus Universitário Darcy Ribeiro, Asa Norte, 70910-900, Brasília-DF, Brasil
guilherme.alencar@unb.br

Abstract. Highway bridges are known as structural systems permanently affected by random loads that can cause significant damage to the structural elements. Nowadays, a challenging problem for structural engineers is associated to the high-stress amplitudes related to the fatigue induced by distortion on the steel elements. Therefore, in this research work, the hot-spot stress method was validated aiming to assess the distortion-induced fatigue strength in welded joints of steel-concrete composite bridges. It is important to emphasize that for the validation of the hot-spot stress method, a full-scale fatigue tests database was taken into account, designed precisely to serve as a basis for the evaluation of the fatigue resistance induced by distortion. This way, the investigated highway bridge finite element model, developed based on the use of the ANSYS program, was utilized as a global model with a local sub model, aiming to perform the compatibility and interpolation of the displacement's fields of both models (global and local). The numerically obtained results based on the hot-spot approach were compared with those calculated with the conventional methods, resulting, therefore, in a considerable difference, showing that the hot-spot method is more realistic, in view of its effectiveness in terms of capture of stress concentrations due to the geometry of welded details, over for evaluation of fatigue damage.

Keywords: steel-concrete composite bridges, fatigue strength, welded joints, hot-spot stress.

1 Introduction

The cause of the fatigue phenomenon in welded steel element connections, which in many cases influence the significant reduction of the service life of metallic structures, is an exceptionally important subject area of study of steel structure engineering. According to the authors Pang et al., Liu et al., Luo et al. and Alencar et al. [1–2], the phenomenon in question is caused by cyclic loads capable of causing failure in the structural system at very low stress levels in relation to the strength limit of the material used.

In the case of mixed (welded) road bridges subjected to vehicular traffic, it is known that their fatigue life is largely governed by the fatigue behavior in the joints of the elements subject to the action of loads [3]. That is, among the weakest points of steel and composite bridges, the welded connections of the elements stand out, since they are responsible for the stress concentrations and responsible for fatigue cracking [4].

Numerical modelling with the finite element method (FEM) is a way of simplifying and determining the localized aspects of welded joints, facilitating local analysis to calculate fatigue life, especially in details with high stress concentrations [5–6]. In this context, appropriate modelling techniques in engineering projects are becoming increasingly important to overcome the problems related to the local approach to structures [7].

The proposed analysis methodology consists of the application of the hot-spot stress method, in order to evaluate the performance to fatigue induced by distortion in welded joints of mixed road bridges (steel-concrete), due to the passage of vehicles on irregular surfaces of the pavement defined by a probabilistic model, including the dynamic actions caused by the vehicles and also the effect of the progressive deterioration of the pavement. In

other words, the method was applied to obtain the stresses in the most critical region or detail of the weld joint from the extrapolation of stresses in neighboring regions, by linearizing the stresses based on the thickness of the element. After that, the service life was determined based on the linear cumulative damage rule and Rainflow counting methods.

However, the main contributions of this study focus on the validation of the hot-spot stress method based on the comparison of the results obtained with those obtained with the conventional methods exposed in the literature, and on encouraging/motivating structural engineers to apply the method in question in welded detail from real case studies, especially on road bridges with real variable amplitude.

2 Vehicle numerical modelling

The truck used in the present research is shown in Fig. 1a, which consists of the AASHTO [8] standard HL-93 fatigue vehicle. The simplified numerical model of the three-axle truck is shown in Fig. 1b, consisting of a system with two main sprung masses (front main block and rear block), and three secondary masses (vehicle axles), located between the spring dampers that simulate the suspensions and the behavior of the tires. The model was developed using the finite element program ANSYS [9]. The mechanical properties, such as: masses, damping and stiffness of tires and suspension systems, are presented in Tab. 1.

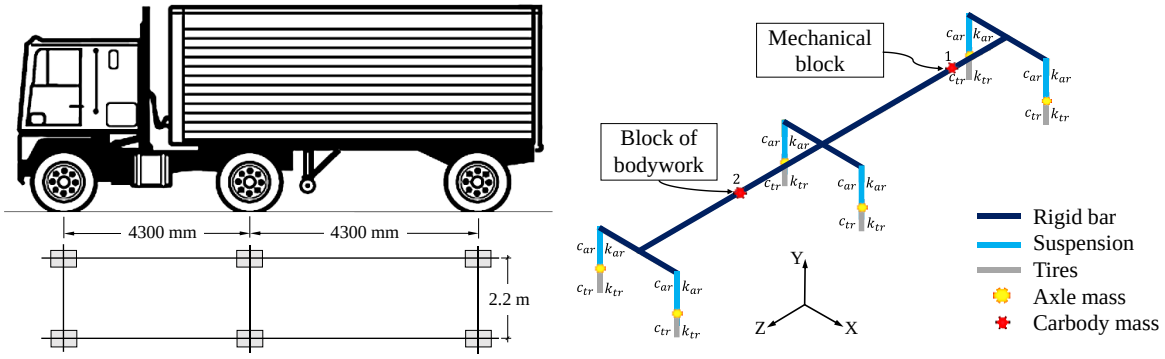

a) Truck geometry: HL-93 vehicle b) Schematic HL-93 vehicle model

Figure 1. HL-93 truck design model: a) standard vehicle from AASHTO [8] and b) FE model in ANSYS [9]

Table 1. Mechanical and geometric properties: HL-93 vehicle model [10]

Parameter	Value	Units	Parameter	Value	Units
Front sprung mass (m_{cf})	2,612	kg	Intermediate tire stiffness (k_{tm})	3,503	N/m
Pitching - Front block rotational inertia ($I_{x,cf}$)	8,544	kg.m^2	Intermediate tire damper (c_{tm})	2,000	N.s/m
Rolling - Front block rotational inertia ($I_{z,cf}$)	2,022	kg.m^2	Rear axle mass (m_{ar})	653	kg
Rear sprung mass (m_{cr})	28,077	kg	Rolling - Rear axle rotational inertia ($I_{z,ar}$)	600	kg.m^2
Pitching - Rear block rotation inertia ($I_{x,cr}$)	181,216	kg.m^2	Rear axle suspension (k_{ar})	1,969,034	N/m
Rolling - Rear block rotational inertia ($I_{z,cr}$)	33,153	kg.m^2	Rear axle damper (c_{ar})	7,182	N.s/m
Front axle mass (m_{af})	490	kg	Rear tire stiffness (k_{tr})	3,507,429	N/m
Front axle suspension (k_{af})	242,604	N/m	Rear tire damper (c_{tr})	2,000	N.s/m
Front axle damping (c_{af})	2,190	N.s/m	Dist. front axle to front block (L_1)	1,240	mm
Front tire stiffness (k_{tf})	875,082	N/m	Dist. front block to center axle (L_2)	3,060	mm
Front tire damping (c_{tf})	2,000	N.s/m	Dist. center axle and to rear block (L_3)	1,925	mm
Central axle mass (m_{am})	808	kg	Dist. between rear block to rear axle (L_4)	2,375	mm
Rolling - Central axis rotation inertia ($I_{z,am}$)	600	kg.m^2	Dist. front block to rear block connection (L_5)	2,673	mm
Central axle suspension (k_{am})	1,903,172	N/m	Dist. between the connection to the rear block	2,312	mm
Center axle damper (c_{am})	7,882	N.s/m	Transverse distance between tires (B_t)	2,200	mm

The HL-93 vehicle finite element model was developed based on the use of the ANSYS software [9] (see Fig. 1b). The vehicle natural frequencies and vibration modes were determined based on a modal analysis performed using the ANSYS program [9], see Fig. 2. This way, the equivalent axle load (ESAL) was calculated taking into account the three axle loads and the vehicle data, based on AASHTO [8] (ESAL = 1.717).

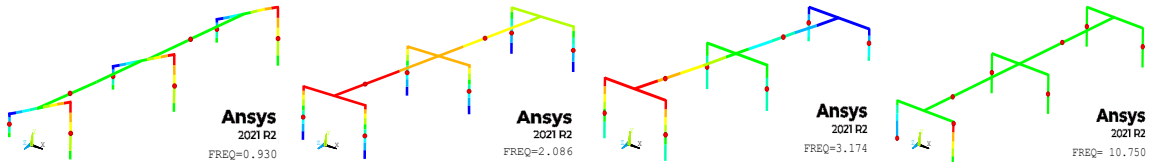

a) f_{01} = 0.930 Hz b) f_{02} = 2.086 Hz c) f_{03} = 3.174 Hz d) f_{04} = 10.750 Hz

Figure 2. HL-93 vehicle vibration modes

3 Modelling of the progressive deterioration for road surface

It is known that road surface roughness is generally defined as an expression of road surface irregularities, and is the main factor that affects the dynamic response of vehicles and bridges [11]. In order to consider the damage to the surface of the runway due to loads, a model of progressive deterioration of the roughness of the runway was needed, which is considered as the International Roughness Index (IRI), assuming values at any time after the start in the surface operation phase of the road (IRI_t).

Based on the studies developed focused on the correlations between the RRC (road roughness coefficient) and IRI indexes, it was possible to use in the present research the relationship between IRI, RRC and IRI_t, as expressed in eq. (1) to (3). The RRC coefficient is used by the International Organization for Standardization [12] to classify the roughness of the track, according to Tab. 2.

$$r(x) = \sum_{i=1}^{N} \sqrt{2\,\Delta\Omega\, G_d(\Omega_i)}\cos(2\pi\ \Omega_i x + \theta_i) \qquad G_d(\Omega_i) = G_d(\Omega_0)_t \left[\frac{\Omega}{\Omega_0}\right]^{-2} \tag{1}$$

$$RRC_t = G_d(\Omega_0)_t = 6.1972\ 10^{-9}\ e^{IRI_t/0.42808} + 2\ 10^{-6} \tag{2}$$

$$IRI_t = 1{,}04e^{\eta t}\ IRI_0 + 263\ (1+ SNC)^{-5}\ (CESAL)_t \qquad (CESAL)_t = f_d\ n_{tr}(t)\ F_{Ei}\ 10^{-6} \tag{3}$$

Where θ_i is the uniformly random phase angle (0 to 2π); $G_d(\Omega)$ is the power spectral density function (cm^3/cycle); Ω_i is the wave number (cycles/m); Ω is the spatial frequency of the floor harmonic i (cycles/m); Ω_0 is the frequency of discontinuity of $1/2\pi$; $G_d(\Omega_0)_t$ or RRC is the road surface roughness coefficient (m^3/cycle); IRI_t is the IRI value at time t; IRI_0 is the initial roughness value right after construction is completed and before opening to traffic (0.90 m/km); t is the time in years; η environmental coefficient (considered 0.1); SNC is the structural number (adopted as 4); $(CESAL)_t$ is the estimated number of traffic in terms of cumulated single axle load equivalent AASHTO 80 kN (18 kip) at time t, in millions; f_d is the design track factor; $n_{tr}(t)$ cumulative number of vehicles passes for future year t, estimated using eq. (4); F_{Ei} is the load equivalence factor for axle category i, calculated strictly following the rules of the AASHTO Guide for Design of Pavement Structures [13].

Table 2. RRC values for road-roughness classification [12]

Road-roughness Classification	Ranges for RRCs
Very good	2 x 10^{-6} to 8 x 10^{-6}
Good	8 x 10^{-6} to 32 x 10^{-6}
Average	32 x 10^{-6} to 128 x 10^{-6}
Poor	128 x 10^{-6} to 512 x 10^{-6}
Very poor	512 x 10^{-6} to 2048 x 10^{-6}

It is worth to mention that CESAL changes according to the traffic annual increase, consequently resulting in a change in the progressive deterioration function. Based on the ADTT and the traffic increase rate per year, they estimated the cumulative number of vehicles passes for the future year t using eq. (4), where N_{obs} is the total number of vehicles in the first year, considered equal to 584,000, due to the location of the bridge within a local road with low truck traffic; and α is the annual traffic increase rate (in this work α = 0% was assumed).

$$n_{tr}(t) = N_{obs}\left[\frac{(1+\alpha)^t - 1}{\ln(1+\alpha)}\right] \tag{4}$$

4 Finite element model of the investigated steel-concrete composite bridge

The investigated structural model corresponds to a mixed steel-concrete road bridge, with a straight axis, simply supported, measuring 13x40 m (see Fig. 3). The system has four steel beams and a 0.225m thick concrete slab. The welded steel elements (A588) have yield strength of 350 MPa and a tensile strength of 485 MPa.

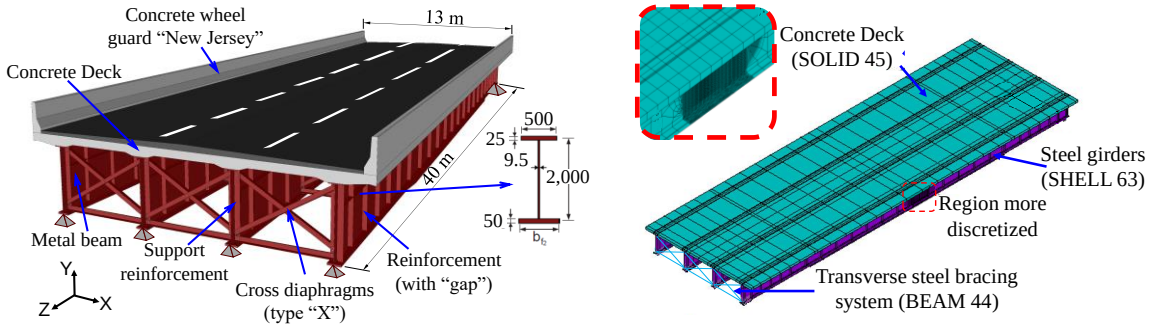

a) Isometric view of the road bridge (units in millimetres) b) Finite element model of the bridge

Figure 3. Investigated simply supported steel-concrete composite highway bridge

The steel-concrete composite highway bridge finite element model was developed based on the usual mesh refinement techniques present in the FEM simulations implemented in the ANSYS [9] program. The FE model adopted used 16,112 elements and 15,550 nodes, resulting in a numerical model with 109,385 degrees of freedom. The bridge natural frequencies and vibration modes were calculated based on a modal analysis performed utilising the ANSYS computational software [9], as illustrated in Fig. 4.

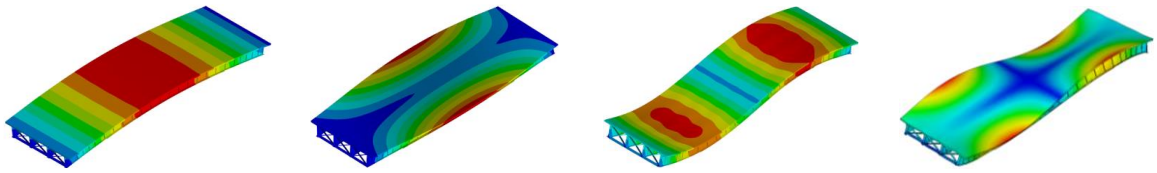

a) f_{01} = 2.970 Hz b) f_{02} = 3.672 Hz c) f_{03} = 9.674 Hz d) f_{04} = 10.872 Hz

Figure 4. Steel-concrete composite bridge natural frequencies and vibration modes

5 Dynamic analysis and fatigue verification with vehicle-structure interaction

The dynamic analysis to solve the problem of dynamic vehicle-structure interaction, considering the effect of vehicle load mobility (HL-93) and road irregularities, was carried out with the help of the MATLAB program. The dynamic equilibrium equations of the vehicle are solved with the direct integration method, and of the bridge with the modal overlap method. The two models were modelled independently, but calculated simultaneously over time. Fig. 5 generically illustrates the vehicle-structure-irregularities interaction.

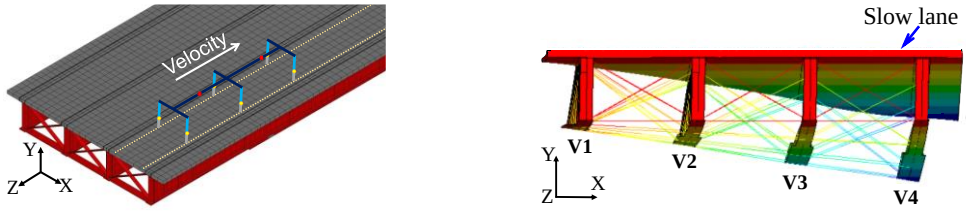

a) Isometric view of the structural system b) Frontal view of the structural system

Figure 5. Three-dimensional model of the vehicle-structure-road irregularity system

This analysis was possible based on the articulation between the MATLAB and ANSYS software. The vehicle-structure interaction including the irregularity was performed in the MATLAB. Fig. 6 illustrates the flowchart with the steps to carry out the fatigue analysis based on the hot-spot stress method in road bridges.

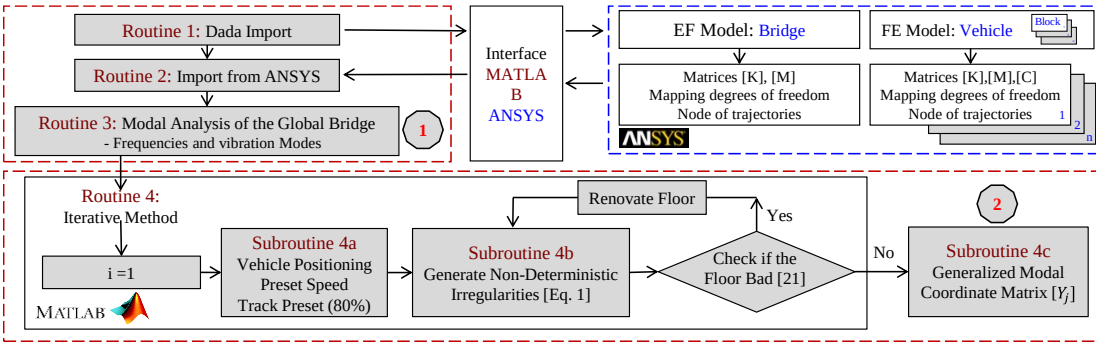

Figure 6. Dynamic analysis flowchart with vehicle-structure interaction including track irregularity.

Fig. 7a illustrates the detail of the case study sub-model for the determination of local stresses. From the stresses of the modal dynamic response of the global FE model of the bridge, it was possible to obtain the modal displacements in the contours of the local detail for each vibration mode (j) and then apply them as displacements imposed on the contour nodes corresponding to the sub-model. Fig. 7b illustrates the flowchart of the analysis to obtain the hot-spot stress acting on the sub-model, taking into account the different vehicle speeds (10 to 60 m/s). The flowchart in Fig. 8 illustrates the steps for calculating the fatigue damage in the most critical region of the sub-model, according to IIW [14].

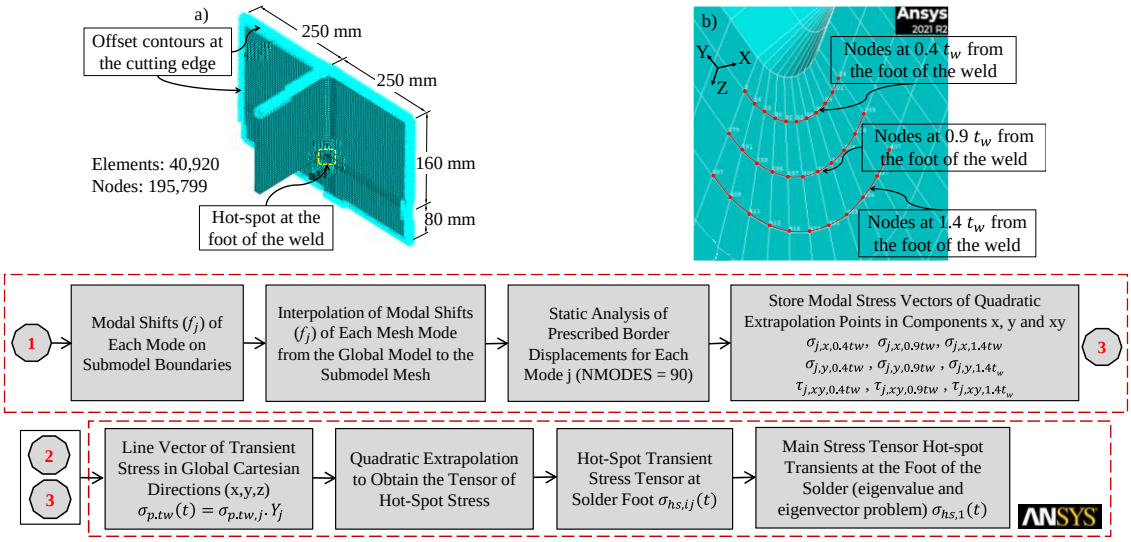

Figure 7. Model and sub-model of the bridge: a) sub-model in FE and b) analysis flowchart in the sub-model

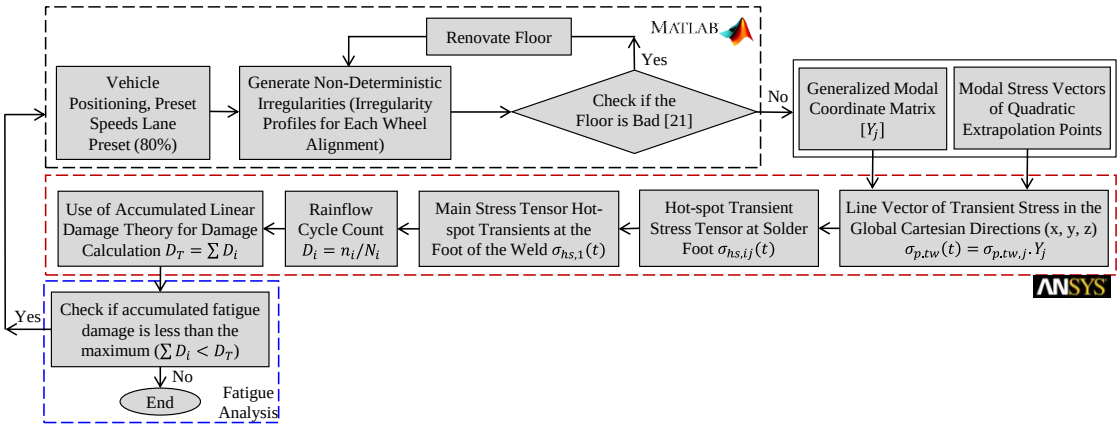

Figure 8. Flowchart with the description of the fatigue analysis and the damage accumulated in the sub-model.

It must be emphasized that after obtaining the stress history based on the finite element software ANSYS [9], the structural response was imported into the fatigue damage accumulation calculation tool ("FatigueCal"), which was developed by Alencar & Correia [15], and then executed for damage assessment.

6 Fatigue assessment

Then, in Fig. 9, the results of the most critical hot-spot stress obtained in the region of the sub-model detail are presented, considering the speed of analysis of the research. It is noteworthy that the hot-spot stress was extrapolated into the three components σ_z, τ_{yz} and σ_y, respectively. However, the principal stress resulting from the combination, σ_1, was obtained at 45 degrees. Fatigue life estimates were based on the Palmgren-Miner rule considering a υ = 50 m/s and traffic growth rate α = 0% and a pavement renovation time interval of 13 years. Fatigue damage was calculated considering surface deterioration over time. Tab. 3 shows the individual and accumulated fatigue damage and the fatigue lives obtained in years, respectively, for the analysed detail. Under these conditions, the fatigue life obtained was 94 years, which is a recommended life in bridge design details, according to the AASTHO standard [13].

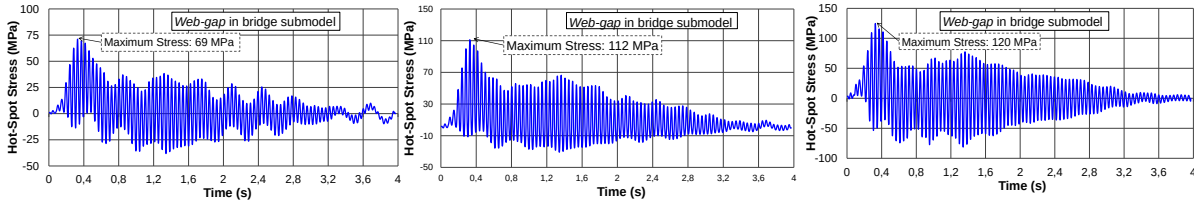

a) Hot-spot stress at z b) Hot-spot stress at yz c) Hot-spot stress at y

Figure 9. Hot-spot stress in the horizontal, oblique and vertical directions in the Web-gap detail: 50 m/s.

Table 3 – Estimate of individual and accumulated fatigue damage due to vehicle passages.

Time (year)	RRC (α= 0%)	Vehicle speed (m/s)						Damage per year	Accumulated damage
		10	20	30	40	50	60		
1	2,1E-06	1,9E-08	1,4E-07	1,1E-08	1,6E-08	1,5E-07	1,7E-07	4,4E-03	4,38E-03
2	2,1E-06	2,0E-08	3,2E-08	1,4E-08	1,2E-08	1,3E-08	1,5E-08	1,4E-03	5,82E-03
3	2,1E-06	6,1E-08	1,4E-08	2,3E-08	1,9E-08	4,0E-08	2,5E-08	1,7E-03	7,55E-03
4	2,2E-06	1,1E-07	2,2E-08	2,3E-08	2,0E-08	1,6E-08	2,4E-08	2,8E-03	1,03E-02
5	2,3E-06	1,2E-07	1,3E-07	1,1E-08	2,6E-08	1,8E-08	2,5E-08	5,8E-03	1,61E-02
6	2,4E-06	4,3E-08	2,5E-08	3,2E-08	3,2E-08	5,5E-08	3,1E-08	1,8E-03	1,79E-02
7	2,7E-06	2,9E-08	3,2E-08	5,6E-08	2,4E-08	2,7E-08	3,2E-08	2,1E-03	2,00E-02
8	3,2E-06	3,0E-07	4,5E-08	6,3E-08	4,0E-08	5,2E-08	5,5E-08	7,3E-03	2,73E-02
9	4,1E-06	1,0E-07	2,6E-08	1,3E-08	4,2E-08	2,3E-07	1,1E-07	2,7E-03	3,00E-02
...	...	...	...	...	...	...	...	...	...
91	2,7E-06	2,9E-08	3,2E-08	5,6E-08	2,4E-08	2,7E-08	3,2E-08	2,1E-03	9,89E-01
92	3,2E-06	3,0E-07	4,5E-08	6,3E-08	4,0E-08	5,2E-08	5,5E-08	7,3E-03	9,97E-01
93	4,1E-06	1,0E-07	2,6E-08	1,3E-08	4,2E-08	2,3E-07	1,1E-07	2,7E-03	9,99E-01
94	6,1E-06	1,5E-07	1,5E-08	3,2E-08	5,4E-08	1,5E-06	2,5E-07	3,5E-03	**1,00E+00**

7 Conclusions

In this study, a dynamic analysis and fatigue assessment was carried out in the structural detail of the beam (V4) of the mixed road bridge, considering the vehicle traffic with speeds from 10 to 60 m/s in the lateral (slow) lane of the road, and with the annual rate of increase in traffic of α= 0% in a period of 13 years, this, based on the recommendations of AASTHO [8]. Thus, the conclusions drawn from the results obtained in this investigation are presented below:

1. A numerical simulation to solve the bridge-vehicle coupled system, based on the 3D dynamics model, was developed in order to determine the transient stress histories due to dynamic loadings.

2. It was possible to conclude that the highest maximum stress amplitude values at the foot of the weld bead in the web-gap detail were observed in the σ_y component, thus resulting in the most critical direction. In addition, it was possible to verify that the highest tensions were caused when the vehicle passed with a speed of 50 m/s.
3. Based on the assumed traffic growth scenario, it was concluded that the analyzed detail reaches its fatigue life limit in the 14th year. In this context, for the detail to reach fatigue failure in 94 years, it would be necessary to renew the floor in the 13th year, as this would extend the life of the bridge by 671%.
4. The values of individual and accumulated fatigue damage were obtained. According to the AASTHO design standard [8], it was found that the detail of the bridge under study presents an adequate behaviour in the face of the fatigue phenomenon. Since the period of 94 years is recommended according to the aforementioned standard, since the same standard in its section 3 (item 3.6.1.4.2), I defined that the project of a bridge must have a useful life at least of 75 years.
5. It is concluded, therefore, that the hot-spot stress method applied in the numerical model was able to clearly determine the fatigue life for out-of-plane stresses, as shown in the present research, which shows the non-limitation in what concerns the delicate local analyses in structural details. Thus, the method in question leads to the most realistic results of welded bridges, as it is able to capture the stress concentrations due to the general geometry of welded details.

Acknowledgements. The authors gratefully acknowledge the financial support for this research work provided by the Brazilian Science Foundation's CNPq, CAPES and FAPERJ.

Authorship statement. The authors hereby confirm that they are the sole liable persons responsible for the authorship of this work, and that all material that has been herein included as part of the present paper is either the property (and authorship) of the authors, or has the permission of the owners to be included here.

References

[1] J. C. Pang; S.X. Li; Z. G. Wang; Z. F. Zhang. General relation between tensile strength and fatigue strength of metallic materials. Mater. Sci. Eng. A 2013, 564, 331–341.
[2] G. Alencar; A. de Jesus; J. G. S. da Silva; R. Calcada. Fatigue cracking of welded railway bridges: A review. Eng. Fail. Anal. 2019, 104, 154–176.
[3] A. Hobbacher. Recommendations for Fatigue Design of Welded Joints and Components; Springer: Cham, Switzerland, 2016; Volume 47.
[4] G. T. Méndez; R. Cuamatzi-Meléndez; A. A. Hernández; S. I. Capula-Colindres; D. Angeles-Herrera; J. C. Velázquez; O. Vazquez-Hernández. Correlation of stress concentration factors for T-welded connections–finite element simulations and fatigue behavior. Soldag. Inspeção 2017, 22, 194–206.
[5] G. Alencar; A. de Jesus; R.A.B. Calçada; J.G.S. da Silva. Fatigue life evaluation of a composite steel-concrete roadway bridge through the hot-spot stress method considering progressive pavement deterioration. Eng. Struct. 2018, 166, 46–61.
[6] Rikeros, D. Fatigue Assessment of Rail Track Detail on Movable Bridge in Estonia Based on 2D/3D Finite Element Modelling Using Hot-Spot Stresses. Master's Thesis, Department of Structural Engineering, Delft University of Technology, Delft, The Netherlands, 2019.
[7] M. Aygül; M. Al-Emrani; S. Urushadze. Modelling and fatigue life assessment of orthotropic bridge deck details using FEM. Int. J. Fatigue 2012, 40, 129–142, doi:10.1016/j.ijfatigue.2011.12.015.
[8] AASHTO. Load and Resistance Factor Design bridge design specifications. Washington, DC: American Association of State Highway and Transportation Officials, 2014.
[9] ANSYS. Advanced Analysis Techniques Guide. Release 20.0 Documentation for ANSYS. ANSYS, Inc., 2021.
[10] P. A. Montenegro; J. M. Castro; R. Calçada; J. M. Soares; H. Coelho; P. Pacheco. Probabilistic numerical evaluation of dynamic load allowance factors in steel modular bridges using a vehicle-bridge interaction model. Engineering Structures, 226(March 2020), 111316. https://doi.org/10.1016/j.engstruct.2020.111316, 2021.
[11] C. J. Dodds and J. D. Robson. "The description of road surface roughness". *Journal of Sound and Vibration*, vol. 31, n. 2, pp. 175–183, 1973.
[12] ISO 8608. *Mechanical Vibration-Road Surface Profiles-Reporting.* International Standard Organization, 1995.
[13] AASHTO. *Guide for Design of Pavement Structures.* American Association of State Highway and Transportation Officials, 2012.
[14] IIW: HOBBACHER, A. Recommendations for Fatigue Design of Welded Joints and Components. International Institute of Welding, doc. XIII-2151r4-07/XV-1254r4-07. Paris, France, 2016.
[15] G. S. Alencar and J. A. F. O. Correia. "A User-Friendly Tool for Fatigue Assessment of Steel Structures According to EUROCODE 3. *New Trends on Integrity*, Reliability and Failure. Porto, Portugal, 2016.